

*Crystal Growth
from
High-Temperature
Solutions*

D. Elwell and H. J. Scheel

Online-Edition of the original book
with additional Chapter II and Appendices A and B



Academic Press London New York San Francisco

A Harcourt Brace Jovanovich, Publisher

Part 014

Please get the complete edition from
<http://e-collection.library.ethz.ch/view/eth:4822>

2011 © D. Elwell & H. J. Scheel

II. Crystal Growth and Liquid Phase Epitaxy of High-T_c Superconductors (HTSC)

11.1. Discovery and Early Developments	635
11.2. Crystal-chemical Aspects	637
11.3. Phase Diagrams and Solubility Curves	639
11.4. Crucible Corrosion	645
11.5. Crystal Growth of High-T _c Superconductors	646
11.6. Pre-requisites for Liquid Phase Epitaxy of HTSC	653
11.7. Effects of Growth Conditions on Growth Modes	660
11.8. Surface Characterization of LPE-grown HTSC Layers	661
11.9. Summary.	664
References	666

II.1. Discovery and Early Developments

Superconductivity was discovered first in metals (e.g. Hg, Pb), then in binary compounds (NbC, NbN, A15-type compounds like Nb₃Sn), and later in ternary compounds like PbMo₆S₈ (Chevrel phases) and BaBiPb-oxides. For many years the highest critical temperature T_c was the 23K of Nb₃Ge, discovered by B.T. Matthias. Then Bednorz and Mueller (1986) found signs of superconductivity at around 30K in a mixture of cuprate phases prepared by solid-state reactions.

Other groups confirmed superconductivity up to 30K in (La, Ba)₂CuO₄, and found T_c up to around 40K in La_{1.85}Sr_{0.15}CuO₄. Later, by crystal-chemical variations like partial replacement of the large cations by Y, Bi, Tl and Hg respectively, T_c was raised to 92K, 115K, 125K and 133K, successively.* These developments are shown in Fig. 11.1 where it can be seen that the chemical complexity, the number of constituent elements of the superconductor, increases with T_c. BCS stands for the Bardeen-Cooper-Schrieffer theory of classical superconductors (Bardeen et al. 1957). The Nobel prizes for the discovery of superconductivity in 1911 by Kammerlingh Onnes, for the BCS theory, and for the discovery of 30K superconductivity in 1986 by Mueller and Bednorz, are indicated by stars.

The problems of material and crystal preparation grow with increasing T_c because the thermodynamic stability ranges decrease. This relation is demonstrated in Fig. 11.2 where the melting or decomposition temperatures of superconductors are plotted. The relatively strong, partially ionic metal-oxygen bonds require the processing of superconducting high-temperature superconductor (HTSC) oxide compounds at sufficiently high temperatures in order to mobilize the species for

* The achievements of high critical temperatures in breakthrough materials have been celebrated as great discoveries. These initial measurements were performed on simply prepared polycrystalline multiphase samples. A very demanding effort of preparing pure phases and crack- and void-free crystals and layers is then required for fundamental studies and for applications of HTSC.

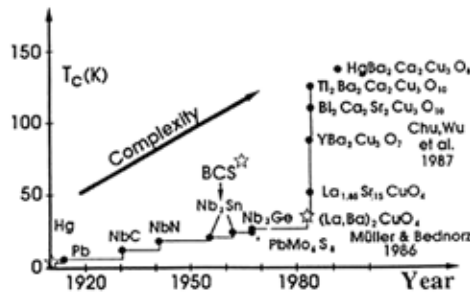


Fig. 11.1. The historical development of superconductors shows that the increasing critical temperatures are observed in compounds of increasing complexity. The awards of three Nobel prizes are indicated by stars, and BCS stands for the theory of classical superconductors by Bardeen, Cooper and Schrieffer 1957 (Scheel et al. 1991).

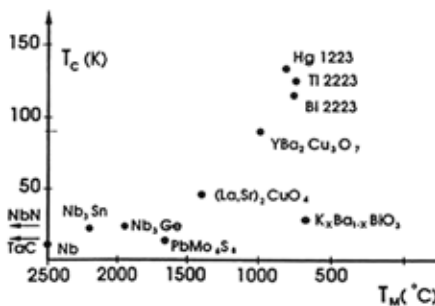


Fig. 11.2. Melting or decomposition temperatures decrease as T_c is increased. This may limit the upper temperature of practically useful superconductivity to about 160K (Scheel et al. 1991)

recrystallization, epitaxial growth, and bulk crystal growth *. From Fig. 11.2. and from the materials engineering problems of the past years it may follow that technologically useful superconductivity may not exceed a temperature around 160 K due to stability limits of HTSC compounds. These limits seem to be related to the phenomenon of high-temperature superconductivity. When this HTSC phenomenon is fully understood, it should be possible to predict and develop practically applicable superconductors with the highest T_c and with a minimum of toxic elements. However, in addition to the basic requirements of the physics, the transformation into practically useful HTSC compounds will demand progress in solid-state chemistry, in crystal chemistry, and in crystal growth technology of the complex compounds where the physics-derived structural elements are incorporated. It may take a generation of scientists and a full multi-disciplinary approach (in contrast to the physics-dominated research in the first ten years of

* Future technologies based on combined HTSC and microelectronic and optoelectronic phenomena will demand HTSC configurations with sufficient stability at processing temperatures and in vacuum.

HTSC research) before novel and useful HTSC compounds can be developed. Until that understanding is achieved, new superconductors will be developed empirically (Abrikosov 1988).

The combined difficulties of complex composition, complex layer structure, and limited thermodynamical stability confront materials scientists and crystal growers with fascinating and unparalleled problems. Some of the problems related to crystal growth and epitaxy of HTSC compounds, with emphasis on the most-investigated $\text{YBa}_2\text{Cu}_3\text{O}_{7-x}$ (YBCO), will be discussed in the following sections.

11.2. Crystal-chemical Aspects

When we define high-temperature superconductivity as the phenomena above the boiling point of liquid nitrogen (77K) for technological applications, or as superconductivity beyond the limits of the classical BCS theory (about 35 to 40K)*, we have four major classes of HTSC compounds. The common features of these are a layer character parallel to the a-b plane, consisting of rock-salt-like A-O layers (with A a large cation like Y, rare earths, Bi, Tl, Hg) and perovskite-like layers B-Cu-O with B being one or two of the alkaline-earth ions Ca, Sr or Ba.

The crystallographic and crystal-chemical aspects of HTSC compounds have been reviewed by Jorgensen (1987), Rao (1988), Sleight (1988), Yvon and Francois (1989), Cava (1990), Goodenough (1990), Raveau et al. (1990) and Park and Snyder (1995), and in numerous books on HTSC. We focus here on a few aspects related to crystal growth. Within the layer structures of the cuprate superconductors there are nearly planar CuO_2 sheets which carry the supercurrent. Uninterrupted continuity of these sheets, or at least excellent percolation, is thus required. The distance between these CuO_2 sheets, as well as localized defects, determine the pinning of the superconducting flux and thus the critical current density and its temperature- and magnetic-field dependence.

Between the CuO_2 layers and the non-superconducting layers exists strain due to lattice mismatch which defines the optimum oxidation state of the copper ions, which should be around +2.2 in p-type superconductors in order to allow Cooper-pair condensation (Park and Snyder 1995). Therefore, for most HTSC applications a compromise has to be found between generally high structural perfection and a high density of localized defects acting as pinning centers for superconducting vortices.

* There is also experimental evidence for phonon-mediated BCS superconductors with T_c below 30K from tunneling spectroscopy and the isotope effect, whereas high- T_c superconductivity above 77K seems more complex and still unexplained.

In addition to YBCO with the superconducting transition temperature $T_c = 94$ K, the Bi-based compounds $\text{Bi}_2\text{Sr}_2\text{CaCu}_2\text{O}_8$ (Bi-2212) and $\text{Bi}_2\text{Sr}_2\text{Ca}_2\text{Cu}_3\text{O}_{10}$ (Bi-2223) and the Tl compounds $\text{Tl}_2\text{Ba}_2\text{CaCu}_2\text{O}_8$ (Tl-2212) and $\text{Tl}_2\text{Ba}_2\text{Ca}_2\text{Cu}_3\text{O}_{10}$ (Tl-2223), have attracted the largest interest for HTSC applications so far. T_c is between 80 and 110K for the Bi-compounds and 112 to 127K for Tl compounds. The layer sequences for the 2212 compounds are:

- BiO-SrO-CuO₂-Ca-CuO₂-SrO-BiO- and
- TlO-BaO-CuO₂-Ca-CuO₂-BaO-TlO-;

and for the 2223 compounds

- BiO-SrO-CuO₂-Ca-CuO₂-Ca-CuO₂-SrO-BiO- and
 - TlO-BaO-CuO₂-Ca-CuO₂-Ca-CuO₂-BaO-TlO-
- for the Bi- and Tl- HTSC compounds, respectively.

The corresponding class of Hg-HTSC compounds was discovered by Putlin et al. (1991) and the critical temperature could be successively raised from 94K (Putlin et al. 1993a), 120K (Putlin et al. 1993b) to 133K (Schilling et al. 1993), the latter in a multi-phase material containing only about 40% of the superconducting phase. The crystal structures have similarity with the analogous series of Bi- and Tl-compounds. As examples of these HTSC-compounds with pronounced layer structure the structural arrangements of the Hg-HTSC compounds Hg-1223 and Hg-1234 with T_c around 130K are shown in Fig. 11.3. a and Fig. 11.3.b, respectively.

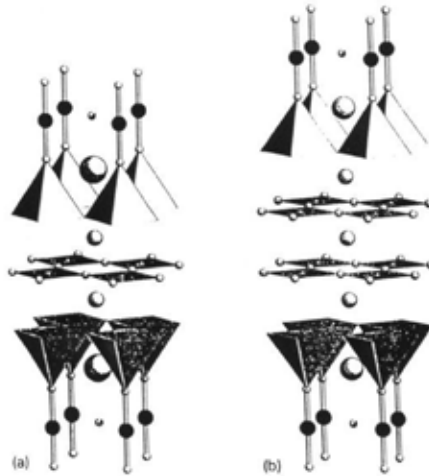


Fig. 11.3. Crystal structures of (a)Hg-1223 and (b)Hg-1234. The large, medium-large, black and smallest circles refer to Ba, Ca, Hg and Cu, respectively. Oxygen is indicated by the second-smallest circles; the partially filled circles in the Hg layer show partially filled oxygen positions. Of the copper-oxygen pyramid only the apical oxygen is represented by circles.

Numerous other HTSC compounds and solid solutions with La, rare earths, and Pb as large cations have been described, also infinite-layer compounds with the stacking sequence - CuO_2 - (Ca, Sr) - CuO_2 -. These compounds are of only fundamental interest to date and will not be discussed here.

The tetragonal or orthorhombic compounds within a class of HTSC compounds have similar a- and b-lattice constants so that stacking of structural units with varying composition may occur depending on local compositional fluctuations during growth. This “*chemical polytypism*” is frequently observed in the Bi-based compounds and can also occur in the other HTSC classes, see Fig. 11.4. Other inhomogeneities in HTSC compounds are due to variations of the alkaline-earth ratios (e.g. Sr : Ca), to mixed site occupancy of Ba and rare earths in the 123 compounds (e.g. $\text{Nd}_{1\pm y}\text{Ba}_{2\pm y}\text{Cu}_3\text{O}_{7-x}$), and to the oxygen content. In addition to oxygen non-stoichiometry, oxygen ordering phenomena can also be observed. All these deviations from the optimum structure, composition and doping have effects on the superconducting properties, as have other common defects like dislocations, stacking faults, twin boundaries, grain boundaries and point defects. Thus, the preparation of structurally and chemically well-defined HTSC crystals and layers is extremely demanding. On the other hand a high density of defects of the size of the superconducting coherence lengths (ca. 5 – 100Å) is desirable to achieve pinning of the superconducting vortices for high-current applications of HTSC. The complex structures and compositions of HTSC compounds open questions about the species in the mobile (liquid or gaseous) phase, about the desolvation and reaction phenomena near the growing surface, and about the incorporation mechanisms.

11.3. Phase Diagrams and Solubility Curves

Thermodynamic data for all possible reactions including redox equilibria, the phase relations around the HTSC phase of interest including its primary crystallization field, and solubility curves with possible solvents are of interest for the optimized fabrication of crystals and epitaxial layers. Data are required for the growth of large crystals, for temperature programs for maximum stable growth rates, and for analysis of segregation in order to achieve crystals of the desired composition and homogeneity. These aspects will be briefly reviewed with emphasis on YBCO and BiSCCO, whereas for other HTSC compounds of importance only a few references will be given.

The thermodynamic data for compounds of the system Y_2O_3 - BaO - CuO have been evaluated theoretically and experimentally, and reviewed by Tsagareishvili et al. (1990), Voronin and Degerov (1991), and Moiseev et al. (1992). The stability limits of YBCO as a function of temperature and oxygen partial pressure, important for the epitaxial deposition and for melt processing, have been ana-

lyzed by Bormann and Nolting (1989) and by Lindemer et al. (1991). This limit can be shifted to higher temperatures by activated oxygen species as shown by Hashimoto et al. (1991). A further effect of oxygen (and of activated oxygen) is to increase all liquidus and solidus temperatures of cuprate systems with increasing partial pressures. This fact has to be taken into account in crystallization processes; it may even be used to program the supersaturation or to achieve growth at the lowest possible temperature.

Of specific interest for crystal growth of the incongruently melting HTSC compounds are phase relations with solvent candidates, with low-melting eutectics such as $\text{BaCuO}_2\text{-CuO}$ for growth of YBCO, the primary crystallization field and the solubility curves of YBCO, and the pseudo-binary diagram YBCO-eutectic.

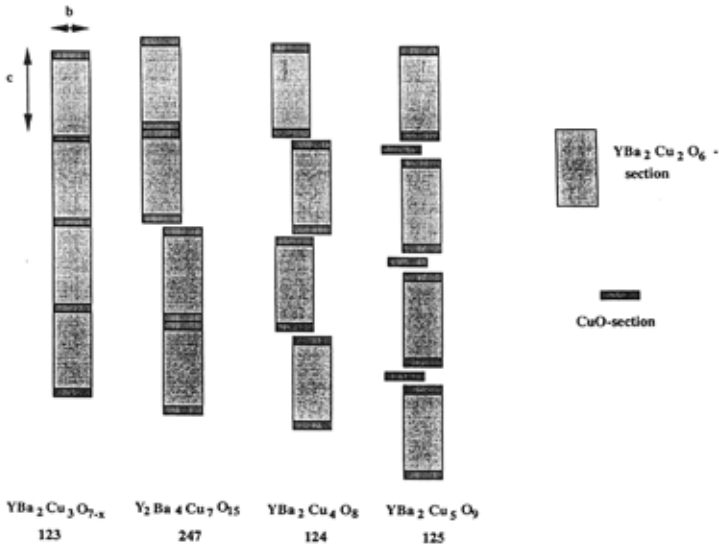


Fig. 11.4. Schematic view of the structures of observed phases in the system $\text{Y}_2\text{O}_3\text{-BaO-CuO}$. The 123 phase (YBCO) is the most widely investigated HTSC-123 compound.

The experimental determination of HTSC phase diagrams is hampered by the following factors in the case of $\text{Y}_2\text{O}_3\text{-BaO-CuO}$ (Scheel and Licci 1991) :

- i) The large differences in melting point of the oxides and oxide compounds : Y_2O_3 2400°C, BaO 1900°C, CuO_x 1140°C in air, $\text{Y}_4\text{Ba}_3\text{O}_9$ 2160°C, and the low-melting eutectics (e.g. 825°C for the $\text{CuO-Cu}_2\text{O-BaCuO}_2\text{-BaCu}_2\text{O}_2$ eutectic).
- (ii) The sluggish reactions typical for peritectic systems, such as slow dissolution of high-temperature phases (once formed) and reaction layers around components which ought to participate in equilibration.

- (iii) The complexity of the quaternary and quinary systems “requiring the preparation of hundreds of compositions and ten times that number of individual experiments” after Roth et al. (1987).
- (iv) The thermodynamically partially open system with valency change of copper and the partial pressure of oxygen as an additional dimension (Holba 1992).
- (v) The very slow equilibration at a given temperature with the actual oxygen partial pressure once melting has occurred, leading to a dense surface of the sample. This causes the presence of non-equilibrium solid and liquid phases.
- (vi) The corrosion of crucibles leading to contamination and shift of equilibria (see below) and to creeping (separation) of liquid phases.

These factors explain the scatter of published HTSC phase diagram data. For example the primary crystallization fields (PCF) from six publications 1987/1988 (see Scheel and Licci 1991) are shown in Fig. 11.5.a along with the proposed PCF in Fig. 11.5.b which is similar to the PCF of Oka and Unoki (1990).

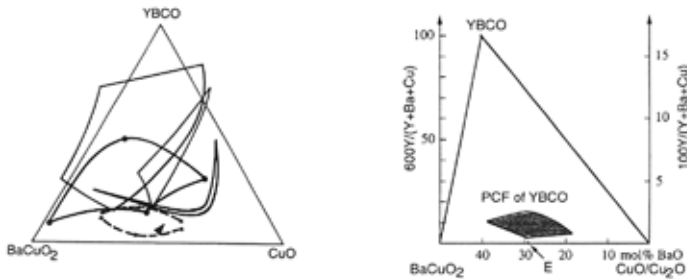


Fig. 11.5. The primary crystallization fields of YBCO in the ternary system BaCuO₂ - CuO - YBCO (a) from different authors (from Scheel and Licci 1991) and (b) as proposed by Holba and Scheel along with the eutectic composition E of the binary BaCuO₂ - CuO in air (Licci et al. 1991).

As solvent for crystal growth and liquid phase epitaxy of YBCO the eutectic composition between BaCuO₂- CuO can be utilized in order to achieve a homogeneous solution (Scheel and Licci 1987). The published eutectic compositions are scattered due to the above-mentioned problems between 18 and 40 mol % BaO, and the eutectic temperatures between 820 and 950°C. Crystal growth experiments followed by flux separation and identification of crystallized phases, in combination with heating curves in differential thermal analysis (DTA), resulted in eutectic temperatures and compositions of 910±10°C / 29±1.5 mol % BaO in air, and 935±10°C / 33±3 mol % BaO in oxygen atmosphere (Licci et al. 1991). These examples of PCF and eutectic composition in the system Y₂O₃ - BaO - CuO

indicate that dynamic methods like DTA and simultaneous thermogravimetry (TG) have to be complemented by long-time annealing- and quenching experiments, by careful examination of reversibility of reactions, and by crystal growth experiments, for determination of liquidus temperatures. Within the PCF of the compound to be crystallized the solubility curve is of special interest for crystal growth and LPE experiments. In Fig. 11.6. the solubility curves for YBCO and for $\text{NdBa}_2\text{Cu}_3\text{O}_{7-x}$ (NdBCO) are compared. Earlier solubility curves are in error because of corrosion of alumina crucibles.

For the determination of HTSC phase diagrams as well as for synthesis of stoichiometric materials and for reproducible crystal growth experiments, the purity of starting chemicals is crucial. Rare-earth oxides, Y_2O_3 , and CuO can be commercially obtained in high purity, i.e. of 99.9 and 99.99% purity of the contained cation. This means that the remaining 0.1% or 0.01 % may be metallic impurities. However, the content of the nominal composition of, say, CuO may be much lower, because of the presence of the cation in other valency states like Cu_2O and Cu , or of volatile anions (sulfate, phosphate etc) or of moisture or organic compounds. Therefore, either essay analysis is recommended or a heat / vacuum treatment adapted for the specific compound. An easy check for crystalline impurity phases is done by x-ray diffraction, of which the detection limit of 0.5% can be achieved (Francois and Scheel 1989) with only 10 to 20 mg of sample. A specific problem exists with the alkaline-earth compounds : carbonates and sulphates

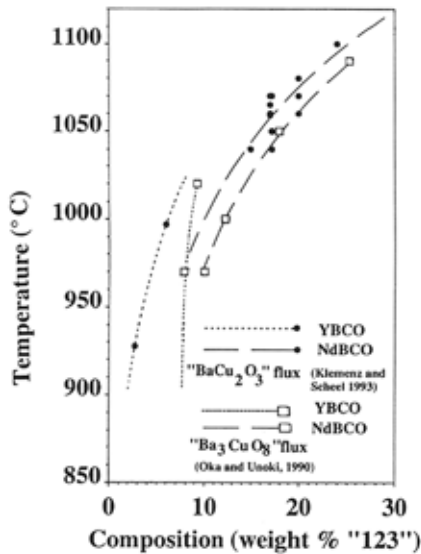


Fig. 11.6 Pseudobinary section in the phase diagrams of YBCO and NdBCO (Klemenz & Scheel 1999)

available as high-purity grades show slow reactivity at typical HTSC synthesis temperatures between 600 and 1000°C. Therefore, BaO or BaO₂ are preferable for synthesis of YBCO, for example. These two oxides are available with purities 95% to 99%, with the main impurities Sr and the reaction products with humidity and with carbon dioxide. Only one source for high-purity BaO₂ could be found*.

For crystal growth of YBCO and other 123- compounds, many solvents well-known for growth of oxide compounds (see chapters 3 and 10) were experimentally tested as the corresponding phase diagrams are lacking. The low-melting fluorides KF and PbF₂ yield only CuO needles. Li- and Ba-borates have relatively high melting points (e.g. Ba₃B₂O₆ 1383°C), above the stability limit of YBCO, however boric oxide may be added in small amounts to any high-temperature solution to use its frequent role in suppressing multinucleation. Lead and bismuth oxides have the disadvantage of significant substitution for Ba and rare-earth ions in 123 compounds. Other common molten solvents like vanadates, molybdates, and tungstates form high-melting compounds with the constituents of HTSC compounds. Only alkali halides have been successfully used for thin crystals of YBCO and of Bi- and Tl-HTSC compounds, and low-melting hydroxides like LiOH or LiOH-NaOH have potential as HTSC solvents (Stacy 1989). These latter solvents probably show low solubilities for the HTSC compounds, thus hampering the growth of large inclusion-free crystals.

Reliable data for the quinary Bi- and Tl-based HTSC compounds require lengthy investigations and become slowly available. The existence regions of liquid plus 2212 and 2223 compounds with the highest superconducting temperatures are so narrow with respect to composition, temperature and oxygen partial pressure, that extreme composition and temperature control are required to synthesize single-phase material and large single crystals (Majewski 1994, Huang et al. 1995, Hallstedt et al. 1996). The solid-solution ranges of the Bi-2212 and -2223 phases are shown in Fig. 11.7.a, and the PCF of Bi-2212 is indicated in Fig. 11.7.b. Solid solutions and the chemical polytypism discussed above are additional complications for the growth of well-defined single-phase crystals and layers.

From the experimental solubility curve, Klemenz and Scheel (1999) determined the heat of solution of YBCO in a solvent with Ba:Cu ratio of 31:69 to be 34.7 kcal/mole. This agrees quite well with data of Tsagareishvili et al (1990). For NdBCO crystals grown in air from the same solvent 28.1 kcal/mole at 1060°C was obtained. Attempts to express the heat of solution using multi-ion or multiple groups in solution have begun (Aichele et al 1997).

*Kojundo Chemical Laboratory Co.Ltd., No. 1-28, 5-chome, Chiyoda, Sakado-shi, Saitama pref, Japan 350-02, (BaO₂ with 0.2 wt % Sr, 0.03 Na, 0.01Si; 0.006 Fe, 0.005 Mg).

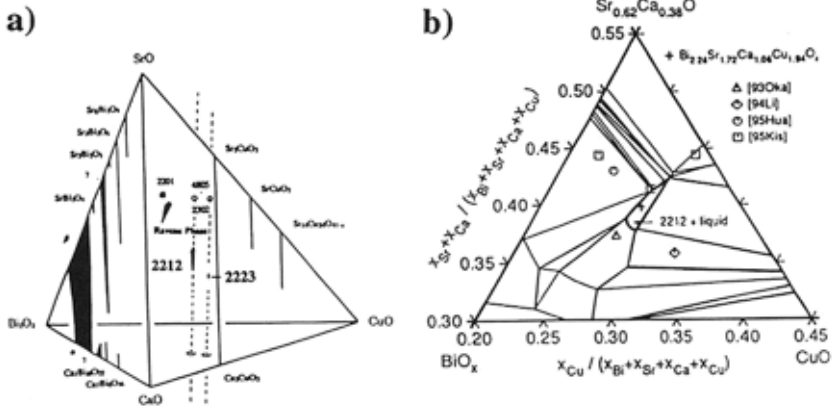


Fig. 11.7(a) Solid solution ranges for Bi-2212 and Bi-2223 in the quaternary system Bi₂O₃-SrO-CaO-CuO at 850°C in air (Majewski 1994). (b) The PCF of Bi-2212 in an isothermal section at 870°C in air (Hallstedt et al. 1996).

The section of the tentative phase diagram Tl₂O₃-BaO-CaO-CuO including the superconducting Tl-2212 and Tl-2223 phases is shown in Fig. 11.8. The very small composition and temperature ranges of the PCFs require both precise temperature control and overcoming the thallium oxide evaporation problem, for phase diagram studies as well as for crystal growth. The toxicity of Tl compounds demands protective measures like gloves, gloveboxes, and well-ventilated hoods. The health hazards of Tl-, and even more of Hg-based HTSC compounds, may limit their applications.

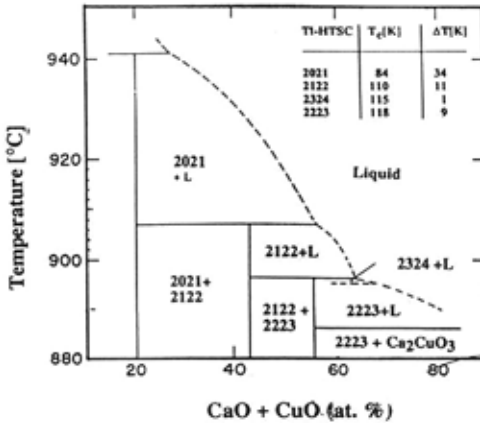


Fig. 11.8. Tentative phase diagram section including the Tl-2212 and Tl-2223 phases with extremely small existence ranges (Kotani et al. 1989). ΔT indicates the temperature ranges of the primary crystallization fields of the Tl-HTSC compounds.

1.4. Crucible Corrosion

In the range of growth temperatures from 850 to 1100°C the BaCuO_2 - CuO and CaCuO_2 - CuO melts for flux growth and LPE of YBCO and of Bi-HTSC phases, respectively, are very corrosive. The low growth rates required to achieve stable growth and bulk crystals free from inclusions (Scheel 1988) lead to very low cooling rates and thus to long runs. This requires crucible lifetimes of several weeks. Crucible corrosion causes contamination of the growth solutions and of the crystals and therefore should be kept at minimum. Platinum crucibles normally used in growth of oxide compounds are heavily attacked, leading to the formation of non-superconducting Pt-rich phases like $\text{Y}_2\text{Ba}_2\text{CuPtO}_8$ (Laligant et al. 1987) and $\text{Y}_2\text{Ba}_3\text{Cu}_2\text{PtO}_{10}$ (Scheel and Licci 1987, Calestani et al 1988). Gold is probably the most corrosion-resistant noble metal. It does show strong wetting and creeping, a fact which can be used to separate the flux from crystallized YBCO (Kaiser et al. 1987). The YBCO crystals grown from gold crucibles typically contain 0.7-0.8 at. % of gold. Also it was observed that Cu diffuses through the gold crucible wall and oxidizes outside, thereby indicating the level of the molten mass inside the crucible (Schmid 1988). Other metal crucibles like iridium or nickel are easily oxidized and alloyed and therefore could not be utilized. Ceramic crucibles consisting of high-melting oxides, having a longer life than Pt crucibles, are also corroded. Alumina crucibles have been widely used in crystal growth and LPE of HTSC compounds. The corrosion mechanism (Scheel et al. 1989) consists of diffusion of Ba and Cu into the ceramic followed by the formation of a reaction layer which is then dissolved by the corrosive crystal growth melt. This corrosion mechanism is similar for zirconia and tin oxide crucibles which had been suggested by Schneemeyer et al. (1987) and by Thomson et al. (1988), respectively.

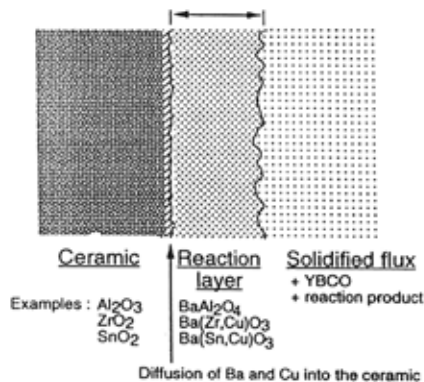


Fig. 11.9. Schematic view of the corrosion mechanism of alumina, zirconia, and tin oxide crucibles (Scheel 1994).

As is indicated in Fig. 11.9, the phases in the reaction layers are BaAl_2O_4 , Cu-doped BaZrO_3 , and Cu-doped BaSnO_3 , respectively, for alumina, zirconia and tin oxide crucibles (Scheel 1994). BaZrO_3 has been tested as a crucible material, and the dissolution rate may be less than that of the Cu-containing BaZrO_3 reaction layer of zirconia crucibles. The apparent low contamination of the crystals may be due to the fact that the contaminated melt passes through the walls of the porous crucible. The low contamination level of the melt remaining in the crucible could be estimated from the flow through the porous crucible walls, the corrosion rate, and from the mass transport by convection and diffusion in the main fraction of the melt. The crucial disadvantage of porous crucibles is the shortened lifetime of the melt, limiting the size and quality of the crystals, or requiring melt replenishment for growth of large crystals. Another porous crucible material with apparently no corrosion is SrIn_2O_4 , discovered by Hoechst in 1989, but crucible development was abandoned when the porosity problem could not be solved. In an attempt to reduce the contamination from crucible corrosion, growth experiments with different BaO-CuO ratios were made and the YBCO crystals analysed for Al content and T_c by Licci et al. (1991b). The molar ratio of 31% BaO / 69% CuO was found to be optimum for both corrosion rate and Al distribution coefficient; Al content was up to 3 at. % on the copper site. T_c above 90K could still be achieved with an optimized oxidation procedure (Licci et al. 1991a).

Crucible corrosion effects could be prevented by development of new crucibles from a high-melting constituent of the HTSC compound to be crystallized, e.g. Y_2O_3 crucibles for growth of YBCO (Scheel et al. 1989). Plasma spraying was used to test new materials without the necessity of full crucible development. Plasma-sprayed yttria layers (Berkowski et al. 1992) on alumina substrates showed 5 to 10 times lower corrosion rates than alumina. Thus yttria crucibles were used for crystal growth (Dembinsky et al. 1990) and for LPE (Klemenz and Scheel 1993) of YBCO and developed by several companies (see Scheel 1994). Similarly the development of Nd_2O_3 crucibles for growth of NdBCO and of CaO crucibles for growth of Bi- and Tl-based HTSC compounds could be envisaged.

Approaches to minimize crucible contamination have been reviewed by Assmus and Schmidbauer (1993). These include skull melting, levitation, and use of a pedestal so that flux can separate to leave small crystals. However, these approaches have not found wide application, mainly because of the long melt life required for growth of large inclusion-free crystals as discussed in the next section.

11.5. Crystal Growth of High- T_c Superconductors

In the first phase after the discovery of superconductivity above 90K in YBCO by Wu et al. (1987), small crystals important for the initial physical investigations

and structure determinations were grown in several laboratories (Kaiser et al. 1987, Laudise et al. 1987, Schneemeyer et al. 1988, Siegrist et al. 1987, Hinks et al. 1987). Mixtures of the constituents of YBCO (BaO , BaCO_3 , Ba(OH)_2 or BaO_2 , with Y_2O_3 , and CuO) with excess of Ba- and/or Cu-constituents were heated in ceramic or gold crucibles to yield a partially liquid mass (slurry). By cooling and solidification, cavities were formed from which small, thin platelets could be recovered. Larger crystals frequently covered the surface of the solidified mass and were then freed by dental drills. In other cases specific shapes of ceramic pieces in crucibles, or the wetting effect of gold were utilized to separate the small YBCO crystals from the flux. There was an apparent limit of thickness and size of the crystals randomly formed in the slurry method.

The first attempts to apply the fundamentals of crystal growth (primary crystallization fields, clean homogeneous solution, control of nucleation and of maximum stable growth rate) were performed at the MASPEC-CNR institute in Parma and at the Electrotechnical Laboratory in Tsukuba. Oka and Unoki (1987) established the primary crystallization field (PCF) of YBCO, later to be confirmed by Holba and Scheel. The decanting of flux from large crystals attached to the crucible wall was reported by Scheel & Licci (1988). The problem with quick decanting is dynamic wetting, the velocity-dependent reduction of the equilibrium wetting angle which leads to flux droplets remaining on the crystal surface. Whereas in normal growth from high-temperature solutions the solvents can be dissolved to free the crystals (see Ch. 3), this has not been achieved in growth of YBCO and other HTSC compounds grown from constituents like BaO-CuO . Therefore, the achievement of clean surfaces still requires special efforts. In specific cases, additives to the melt may increase its surface tension and thus the wetting angle. Another method is to approach the equilibrium wetting angle by very slow removal of the melt (or of the crystal) by suction: a porous ceramic piece is introduced into the melt containing grown crystals to slowly withdraw the liquid (Boutellier et al. 1989).

Thin platelets were generally formed in the early phase of YBCO crystallization, typical thicknesses being 10 to 100 μm with lateral dimensions up to 3mm. From the crystallographic structure of YBCO, with a layer character parallel to (001) but with strong bonds along [001], a more equidimensional shape is expected as equilibrium habit. In early 1988 the formation of thin YBCO platelets was explained by morphological instability, as a form of unstable growth similar to dendrites (Scheel 1988). A comparison was made with the thin plates found in cubic or nearly cubic perovskites, where the large growth anisotropy was explained by the twin-plane reentrant-edge mechanism or by a large number of screw dislocations (see Ch. 5). The answer for YBCO platelets was revealed by an investigation using combined scanning-electron microscopy (SEM) and scan-

ning tunneling microscopy (STM). The narrow (100) surfaces showed remarkable deviations from flatness as indicated schematically in Fig.11.10.a.

The left side of the 76 μm wide surface is raised with respect to the right side by about 3 μm ; we call this the *leading edge*. The initial steep slope of about 4.5° changes at a line indicated by arrows to a slope of 2.8° and, in the middle of the surface, to a slope of 2.1° . The surface rises again to the right-side edge which we call the secondary edge. The profiles of this platelet and of a 53 μm thick YBCO platelet are shown with exaggerated angles in Fig. 11.10.b.

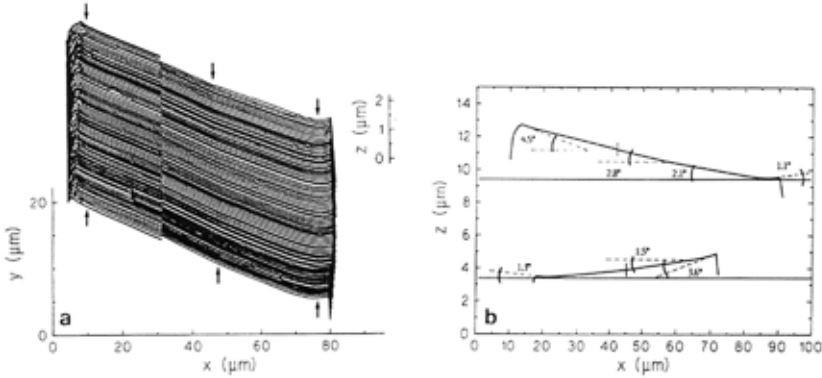


Fig. 11.10. (a) An edge-to-edge STM plot of a (100) face of a YBCO crystal S46. The changes in slope are indicated by arrows. (b) Profiles of the (100) faces of the crystals S46 (top) and S61 indicating the different slopes with respect to the horizontal lines representing the crystallographic (100) planes. The angles are exaggerated due to the different scales in x and z. (Scheel and Niedermann 1989).

In this leading-edge growth mechanism the raised edges appear to act as elongated dendrite tips. The steps originating from these rough edges propagate downwards towards the lowest region where they are annihilated by steps arriving from the secondary edge. Note that the supersaturation profile, due to the varying diffusion-boundary layer thickness across the (100) surface, is not compensated by a continuous change in slope, but by discrete slope changes along the lines indicated by markers in Fig. 11.10.a.

Remarkable deviations from the flatness of narrow faces of platelets have been observed with other materials (Licci and Scheel, unpublished). Platelets appear to occur in cases of structurally induced growth anisotropy (layer structures) or are caused by either the twin-plane re-entrant-edge mechanism (see Ch. 5) or by the leading-edge mechanism. When the latter is fully understood, a process for reproducible fabrication of platelet crystals (for substrates etc.) may be envisaged.

Since platelets of YBCO are a form of growth instability, a low supersaturation and very low cooling rates should result in development of the equilibrium habit.

This has been confirmed by Sadowski and Scheel (1989) as shown in Fig. 11.11. Crystals of more than 5 mm thickness have now been grown, the main problem being contamination from the crucibles. Another problem is oxidation of the as-grown tetragonal $\text{YBa}_2\text{Cu}_3\text{O}_6$ to the orthorhombic, superconducting $\text{YBa}_2\text{Cu}_3\text{O}_{7-x}$ phase with x between 0.0 and 0.1. This problem has still to be solved in order to achieve large (cm^3) superconducting crystals for fundamental physical studies such as neutron scattering. The oxidation of a compact YBCO crystal is complex: 1) due to the structural phase transition and the related large changes in the lattice constants, 2) due to the large differences of the oxygen diffusion coefficients in the three orthorhombic directions, and 3) due to the strains caused by the gradients since the oxidation starts from the periphery of the crystal. The strains are partially released by twinning. It is a challenge to design an oxidation procedure (with programming of temperature, oxygen fugacity, uniaxial pressure) to yield large single-domain fully oxidized crystals of YBCO free of cracks and micro-cracks; then it would be worthwhile to grow large YBCO crystals to be oxidized for fundamental measurements.

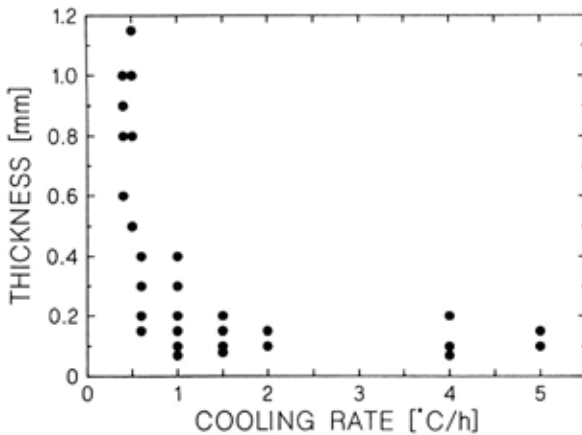


Fig. 11.11. Experimentally observed YBCO plate thicknesses for various cooling rates (Sadowski and Scheel 1989).

Alternative approaches to grow HTSC crystals are the *travelling-heater method* (THM) and the *travelling-solvent method* (TSM) introduced in Chapter 7. For the incongruently melting HTSC compounds, either solvents or non-stoichiometric melts, with excess constituents acting as solvents, have to be applied. The major advantage of THM and TSM is the fact that these techniques are crucible-free, thus eliminating contamination of the crystals through crucible corrosion. However, the technological difficulties have so far prevented the successful application

of THM/TSM to HTSC compounds (Revcolevschi and Jegoudez 1996). These include instability of the liquid zone and of the growth interface, crystal size limitation, and difficulty to achieve single-crystallinity and phase purity. Recently TSM was improved to yield quite large crystals of NdBCO (Kuroda et al. 1997).

Top-seeded solution growth (TSSG) has the disadvantage of contamination from crucibles and growth instability, though by rigorous application of the principles discussed in Chapters 6 and 7 it should be possible to grow large ($>1 \text{ cm}^3$) inclusion-free crystals of most HTSC compounds. Relatively large crystals of YBCO have been TSSG-grown by Zhokov and Emelchenko (1993).

For application of large HTSC crystals in magnetic bearings the perfection requirements are not so stringent. Secondary phases and other defects are useful to enhance the critical current density by fixation of the superconducting vortices. Crystals are grown by Bridgman-like solidification (melt-texture-growth process; Jin et al. 1988) or from peritectic melts with source material: a combination of TSSG and gradient transport. The special problems in development of bulk "imperfect" HTSC crystals are reviewed by Murakami (1992), Alexander et al. (1992), Yamada and Shiohara (1993) and by Wang et al. (1996).

Whisker- and needle-shaped crystals of NdBCO have been grown by Klemenz and Scheel (1999). Crystals up to 2 mm in thickness and 7 mm in length were grown by holding a NdBCO/BaO/CuO melt at 1045°C for a week in a neodymium oxide crucible. Dissolution of the crucible wall provides the supersaturation. The crystals were separated by decanting the residual melt and allowing the crucible to disintegrate at room temperature on exposure to moisture in the air. The superconducting transition in the crystals occurred at 77K, below the maximum for NdBCO because of the replacement of some barium by excess neodymium. Whiskers may be useful as the base for superconducting wires and tapes.

The highest T_c materials, those of Bi, Tl or Hg, were discovered in mixtures of phases made by solid-state reactions. The discovering groups never identified the superconducting phase or grew single crystals, and it was left to other groups to perform these more challenging tasks, as in the case of the discovery of LaBaCuO and YBaCuO HTSC materials.

Crystal growth of the Bi- cuprates has been attempted by flux growth using alkali halides as solvents, or by using excess constituents as solvents. Soon after the discovery of the Bi- HTSC compounds the growth of crystals was attempted in numerous laboratories (Liu et al. 1988, Hidaka et al. 1988, Schneemeyer et al. 1988, Hikita et al. 1988, Katsui and Ohtsuka 1988, Ginley et al. 1988, Ciszek et al. 1988, Nomura et al. 1988, Ren et al. 1988, Takekawa et al. 1988, and others). Thin platelets generally consisting of several Bi- phases like $\text{Bi}_2\text{Sr}_2\text{Ca}_1\text{Cu}_2\text{O}_{8+x}$ (Bi - 2212), Bi - 2223, Bi - 2112, and Bi 2201 were obtained. By cleaving, thin single-crystalline plates up to a few micrometers in thickness could be achieved. The

growth of large single-phase crystals is difficult due to the narrow temperature stability ranges (Komatsu et al. 1992). Additional problems include very small primary crystallization fields (which become only slowly known), and the intergrowth of the structurally similar compounds (in the a-b plane), which was named chemical polytypism (Scheel 1994) or syntactic intergrowth (Morosin et al 1988).

Developments in the growth of the Bi - HTSC compounds Bi - 2201, Bi - 2212 and Bi - 2223 until 1993 have been reviewed by Assmus and Schmidbauer (1993), and the growth by THM / TSM by Revcolevschi and Jegoudez (1996). A special problem was the achievement of single-phase crystals of the Bi-2223 phase. 97% pure crystals of Pb - containing Bi - 2223 were obtained by a "fused - salt reaction method" using excess KCl as flux (Chu et al. 1992; Chu and Mc Henry 1997).

Fiber crystals of HTSC compounds may find applications in current-carrying structures. The laser-heated pedestal growth method was used to grow thin crystalline rods of Bi- HTSC compounds 0.25 to 1mm in diameter (Feigelson et al. 1988; Gazit and Feigelson 1988). With growth rates of 5 mm/hour and feed rods of 1.2 mm diameter, polycrystalline textured fibers were obtained. For a certain length of growth the melt composition adjusts to steady-state growth. However, it would be difficult to achieve single-phase and single-crystalline fibers due to the narrow thermodynamic stability limits of the HTSC compounds. Whiskers of lead-doped Bi-2212 could be obtained from a glassy (melt-quenched) plate heated at 840°C for 120 hrs in a stream of oxygen gas; whereas the same treatment of polycrystalline material did not yield any fibrous crystals (Matsubara et al. 1989).

Single crystals of the superconducting phases of the system Tl-Ba-Ca-Cu-O would be of special interest, due to the high critical temperatures of several phases with minor structural differences, for fundamental investigation of the mechanism of high-temperature superconductivity. According to Paranthaman et al. (1992) there could be four TlBaCaCuO phases with T_c above 100K. Following the tentative phase diagram (see above) of Kotani et al. (1989), the peritectic decomposition temperatures of the TlBaCaCuO phases are very similar, between 893° and 941°C, so that the temperature intervals for growth within the primary crystallization fields are very small. Thus the growth of large crystals of the pure Tl-phases is extremely difficult, though not impossible when the scientifically derived growth conditions are established. Another difficulty is decomposition of Tl_2O_3 to the volatile Tl_2O and oxygen, so that synthesis and growth should be performed in sealed ampoules, preferably at elevated pressure. The effect of the oxygen (partial) pressure on liquidus, peritectic and eutectic temperatures has to be considered. Another obstacle is the toxicity of volatile Tl compounds, which require handling in gloveboxes or well-ventilated hoods, with eye and skin protection, and prevention of inhalation. Yet another problem is connected

with the layer structure of the Tl-phases which, in conjunction with the narrow existence ranges of the phases, leads easily to chemical polytypism, so that the preparation of large single-phase crystals of the various Tl-phases has not been achieved. The typical procedure of growth of platelets of the Tl-phases of a few mm lateral dimensions and about 0.1 mm in thickness consists of introducing the starting materials into a gold tube or gold foil, and bringing this into a sealed platinum crucible or alumina tube. This arrangement is heated to 930°C for one to two hours and then step-cooled to 870°C for the growth of Tl-2212, 2201 and 2223 phases (Venturini et al. 1991, Liu et al. 1990, Duan et al. 1992). Normally, an excess of constituents is used, for instance $Tl_2O_3 + CuO$ or $CaO + CuO$, in order to enhance crystalline perfection. The crystals are then recovered mechanically and by cleaving from the solidified melt. Further details on Tl-phase crystallization can be found in the reviews of Assmus and Schmidbauer (1993) and of Paranthaman et al. (1992). However, a reliable analysis of the phase relations and of the primary crystallization field, and its use for an extremely well-controlled crystal-growth experiment with control of nucleation, supersaturation and stable growth rate, has not yet been reported.

After the synthesis of complex $HgBa_2RCu_2O_7$ compounds (with $R = Y$ or rare-earth ions) by Putilin et al. 1991, the highest-known T_c superconductors based on $HgBaCaCuO$ phases were discovered at Moscow State University (Putilin et al. 1993 a, 1993 b). In an attempt to reproduce the Hg-based phases (Schilling et al. 1993) the silica glass ampoule broke, leaving a poly-phase mass containing about 40 % of superconducting phase with T_c 133.5K. By transmission electron microscopy they found evidence for Hg-1212 and Hg-1223 phases, and it was established by Adachi et al. (1993) that the Hg-1223 phase was the compound with T_c above 130K.

The preparation of single crystals of Hg-based superconductors has been hampered by the low thermodynamic stability of HgO and other Hg-compounds. Related problems are the high mercury and oxygen pressures, requiring high-pressure work in small containers, and the toxicity of Hg vapors, requiring special safety precautions. The size of Hg-HTSC crystals has not yet passed 1 mm: Hg-1223 (Finger et al. 1994, Colson et al. 1994), Hg-1234 (Schwer et al 1995). By partial replacement of Hg by Bi, small crystals with T_c up to 131K were synthesized at ambient pressure by Pelloquin et al. (1996 a, b). The Bi_2O_3 is considered to act as a solvent.

This section has shown that the difficulty of crystal growth of HTSC compounds increases with the complexity of composition, and with decreasing thermodynamic stability, as indicated with Figs. 11.1 and 11.2. Further problems are due to the high vapor pressures of Bi-, Tl- and Hg-oxides, the non-availability of convenient solvents, and the lack of reliable thermodynamic data and phase

relations. Large crystals of, say, cm^3 size could in principle be grown of most of the HTSC compounds with T_c above 77K. However, this would require a careful collection of the above data, a theoretical analysis of the necessary crystal growth conditions based on the fundamental aspects discussed in this book, and a systematic approach to fulfil these conditions. This would include precise control of the relevant crystal growth parameters.

Another problem in crystal growth of the superconducting phase, which has been referred to above but not treated in detail, is that of oxidizing the as-grown tetragonal to the orthorhombic superconducting phase. Oxidation without crack formation is the limiting factor for achieving large high-quality crystals and LPE layers of the superconducting orthorhombic phase of YBCO. As stated above, the tetragonal form of YBCO with oxygen deficiency x around 0.8 has to be oxidized to a value of x in the range from 0.1 to zero. The transformation to the orthorhombic phase on oxidation and cooling occurs at about 650°C. The splitting of the tetragonal a axis to the orthorhombic a and b axes, together with a discontinuous change in the c axis, leads to strain which, for small crystals, can be relieved by twin formation. However with increasing crystal and layer size and crystallographic perfection, cracking is normally observed as the means of relieving strain. This problem is enhanced by the extremely slow oxidation kinetics, requiring long anneals, and by significant anisotropy of the oxygen diffusion found not only in directions parallel and perpendicular to the c axis (by a factor of $\sim 10^6$), but also within the ab plane (by a factor $\gg 10^2$) (Rothman et al 1991). The oxidation is further hampered by contamination of the crystals, for example by Al from the alumina crucibles. Solving this problem by systematic experiments would require excessive time and the destruction of many high-quality crystals and layers. Therefore an alternative approach is preferable, which still requires extensive data on the temperature dependence and anisotropy of the diffusion, also on the lattice constants and mechanical properties of YBCO. The problem may be reduced by changing from the more popular YBCO to NdBCO or LaBCO, which have similar superconducting properties but smaller orthorhombicities, i.e. smaller differences between a and b lattice dimensions.

11.6 Prerequisites for Liquid Phase Epitaxy of HTSC

Superconducting tunnel devices, especially for digital applications and SQUIDS, need homogeneous layers and multilayer structures with very flat surfaces. In view of the very short coherence lengths of the cuprate superconductors, only smooth surfaces on structurally “perfect” layers allow the use of planar technology. The very demanding requirements for planar devices include reproducible etching characteristics and a very small spread in the device characteristics. If

the layers are very flat and structurally of high perfection, high device yields are possible.

Major efforts have been made in perhaps a thousand groups worldwide working in physical vapor deposition (sputtering, pulsed laser deposition, molecular beam epitaxy, etc). In addition, there are several groups working on chemical vapor deposition, and about 10 groups working in liquid phase epitaxy. So far, the required surface flatness has not been achieved. The first single crystal YBCO layers with flatness approaching device requirements were reported by Klemenz and Scheel (1993) and by Scheel et al (1994). The critical factors determining perfection and surface morphology will be reviewed here. Nucleation and growth modes will be described briefly, and the major problems will be outlined. A more detailed discussion of the control of epitaxial growth modes is given in Appendix B.

The most important parameter determining nucleation and growth modes is the chemical potential, usually expressed in terms of the supersaturation, as the driving force for epitaxial growth. The supersaturation is best expressed as

$$\sigma = (n - n_c) / n_c = \Phi \Delta T / RT^2 \quad (11.1)$$

with n and n_c the actual and equilibrium concentration of solute, Φ the molar heat of solution, ΔT the undercooling, R the gas constant and T the deposition temperature. For LPE, the Gibbs free energy difference is about 40 +/- 10 kcal/mole, compared with about 600 kcal/mole for vapor growth. This large difference leads to growth by macroscopic spirals and step propagation over large distances in LPE, versus two-dimensional nucleation and spiral islands in vapor growth. The average lateral distance between steps is correspondingly 0.5-10 μm in LPE, and 20-50 nm in vapor growth.

The misfit between the YBCO layer and the substrate at the growth temperature also has an important influence on the surface nucleation and growth modes. Misfit reduces layer-by-layer growth and enhances two-dimensional nucleation (island formation) and localized step flow. Thus the misfit acts in the same direction as a high supersaturation, and the supersaturation needed for growth increases with misfit. The effect of misfit on the growth mode is shown by the trends in Fig. 11.12. Most substrates used in vapor growth have a misfit of at least 0.1%, and some up to 8%, so the layer-by-layer growth mode is excluded. The critical layer thickness for crack propagation is shown as a function of misfit in Fig. 11.12. The strain caused by misfit at the growth temperature, and on cooling due to thermal expansion differences, may be partially or completely relaxed by the formation of misfit dislocations, by microcracks, or by macroscopic cracking. The dominant stress relaxation mechanism depends on the elastic strain acco-

modation, and on the oxidation- and phase transition-induced strain discussed in the previous section. When the distance between the misorientation steps is less than about 19 times the critical nucleus, two-dimensional nucleation can be suppressed in favor of a very high step density (Lupo et al 1993). All these factors influence the superconducting properties, especially flux pinning and the critical current density and its field dependence. It is surprising that these materials engineering problems have received little attention to date.

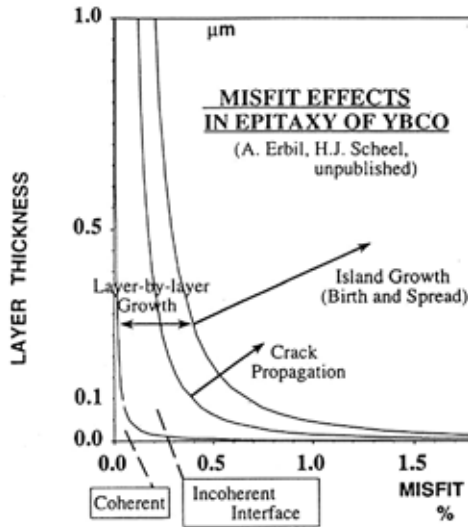


Fig. 11.12. Effect of substrate misfit on the growth mode, interface structure and crack propagation as a function of layer thickness (Erbil & Scheel, unpublished).

The mode of growth can be best assessed using morphological studies of the surface of the layers deposited, as discussed in more detail in Section 11.8. The most powerful methods of surface examination are scanning tunneling microscopy (STM) or the related atomic force microscopy (AFM), and the Nomarski differential interference contrast optical microscopy (DIM). The origin of macroscopic growth spirals in crystal growth from high temperature solutions was found to be screw dislocations, as discussed in Chapter 4. In contrast, the occurrence of spiral islands in PVD and CVD layers, in concentrations of 3×10^8 to over 10^9 per cm^2 , is not yet clear. The spiral density corresponds to the concentration of two-dimensional nuclei, so that a model based on coalescence of slightly tilted islands (Scheel 1994; Stowell 1975) is the most likely explanation. Fig. 11.13 shows small spiral islands typical for vapor growth, compared with typical macroscopic

growth spirals seen in LPE. The largest inter-step separation, $17\ \mu\text{m}$, was seen on layers grown by LPE (Klemenz and Scheel 1993).

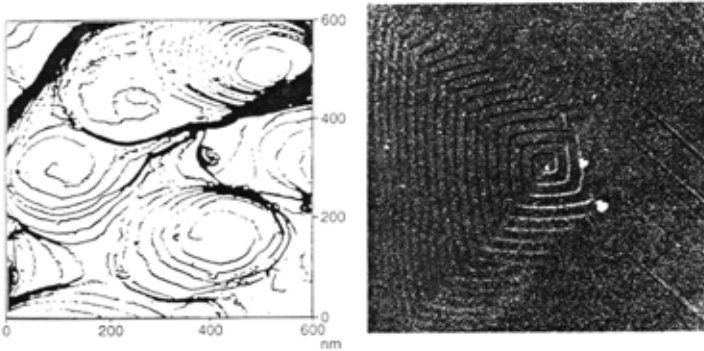


Fig. 11.13. Typical spiral structures of (a) vapor-grown and (b) LPE-grown YBCO layers. Scales are different to correspond to $>3 \times 10^8$ islands per cm^2 in vapor growth and about 10^3 per cm^2 in LPE-grown layers (Scheel 1994).

Substrates play a significant role in the epitaxial growth of YBCO and related compounds. In addition to misfit, misorientation and thermal expansion, substrates must fulfil other requirements. Chemical and thermal stability, lack of structural transitions causing twinning (so excluding most perovskites), application-specific microwave and dielectric properties, mechanical strength, and affordability and machinability are all significant factors in substrate selection. Since substrates which meet all these requirements have not yet been developed, an alternative approach consists of buffer layers on low-cost substrates such as silicon or sapphire, or on polycrystalline substrates such as steel. Another alternative is graphoepitaxy, i.e. substrates with artificial surface structures such as grooves or island depressions (Givargizov et al 1982), or “structural graphoepitaxy” where the surface has regular corrugations due to the crystallographic structure, which control the epitaxial orientation of the superconductors (Miyazawa & Mukaida 1994).

Fig. 11.14 shows some widely used substrates with the temperature dependence of their lattice constants. Also shown are data for YBCO, with the tetragonal-orthorhombic transition. The misfit tolerance at the epitaxial growth temperature is less than 0.1%, and the thermal expansion difference between the HTSC layer and the substrate should be less than 20%. None of the substrates in Fig. 11.14 meets these requirements. In fact, the misfit is usually above 1% so that, in principle, flat surfaces and layer-by-layer growth cannot be expected (Grabow & Gilmer 1988).

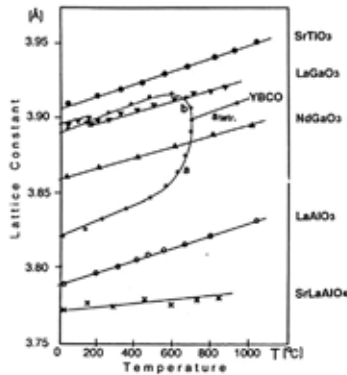


Fig. 11.14. Lattice constants and thermal expansion of some important substrates, compared with YBCO. MgO and ZrO_2 are off scale.

Klemenz et al (1999) reported the growth of YBCO on (110) $NdGaO_3$ substrates where the misfit is 0.28%. A supersaturation of 0.03, corresponding to an undercooling of 3K, was found to be required for c-oriented films; higher supersaturations result in a transition to a-axis growth. At lower supersaturations, the driving force for crystallization is too small to compensate the misfit strain effects, and there is dissolution of the substrate. The Nd^{3+} ions from the substrate are then incorporated by deposition of (Y,Nd)BCO. Under these conditions the growth of a-axis material is favored. This was confirmed by earlier work on $NdGaO_3$ substrate etching and formation of the solid solution layers (Dubs et al 1995; Sandiumenge et al 1994). Table 11.1 compares the misfit at ambient temperature and at 1000°C for YBCO on (110) $NdGaO_3$, with subscripts L and S used to denote the layer and substrate respectively; d_s is $[110]/2$, c_L is $[001]/3$, and $\tan \Delta\gamma$ is the out-of-plane angular misfit. In epitaxy, the minimum supersaturation for growth increases with misfit. Therefore, the distance d of misfit dislocations is proportional to the size of the critical nucleus. For deposition at a supercooling of 3K, $\rho_c = 27$ nm for the ac orientation transition of YBCO on $NdGaO_3$, and the average misfit is 1.3%.

Fig.11.15 shows the relation between the radius of the critical nucleus and the supersturation, and it can be seen that the misfit is approximately equal to the radius of the critical nucleus r_s^* . For deposition at a supercooling of 3K, $r_s^* = 27$ nm for the ac orientation change. In this case, the misfit approximately cancels the thermodynamic driving force for 2-dimensional nucleation. Low supersaturation favors c-oriented nuclei since the lattice match is better. A complete understanding would need calculation of elastic and interfacial energies as a function of geometry, anisotropic strain, and the size of the critical nucleus.

For an Archimedian spiral, the step separation for monomolecular steps is $4\pi r_s^*$ or $19r_s^*$ (see Appendix B). Thus the achievement of 10 μm step separation, as required for reproducible Josephson tunnel devices, needs a supersaturation of $<0.17\text{K}$ and a misfit of $<0.08\%$. These conditions are difficult to meet, but LPE offers a much better chance of meeting these goals than vapor deposition.

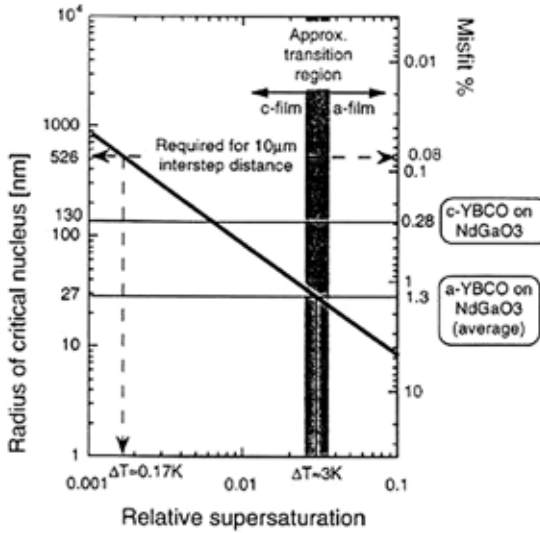


Fig. 11.15. Radius of critical nucleus as a function of supersaturation for YBCO on NdGaO_3 , also showing corresponding misfit.

YBCO on (110) NdGaO_3	misfit at 1000°C	misfit at 25°C
c-film :		
$a_L \parallel d_S / b_L \parallel c_S / \tan \Delta\gamma$	0.28 / 0.25 / 0.5	-1.03 / +0.76 / 1.3
$b_L \parallel d_S / a_L \parallel c_S / \tan \Delta\gamma$	0.28 / 0.25 / 0.5	+0.57 / -0.84 / 1.3
a-film :		
$c_L \parallel d_S / b_L \parallel c_S / \tan \Delta\gamma$	2.59 / 0.25 / 0.5	+0.72 / +0.76 / 1.3
$c_L \parallel d_S / a_L \parallel c_S / \tan \Delta\gamma$	2.59 / 0.25 / 0.5	+0.72 / -0.84 / 1.3

Table 11.1 Misfit of observed orientations at 1000 and 25°C for YBCO on NdGaO_3 .

Fig. 11.16 shows the corresponding requirements for substrate misorientation, together with the experimental example. The substrates used in the experiments described above had misorientations of 0.2 to 0.5°. The supersaturation is, of course, only valid for the specific system but similar values are expected for comparable HTSC LPE systems. For higher supersaturations, step bunching was observed, and can be avoided in this example only if the substrate misorientation is extremely small, about 0.02. This is another very challenging requirement for the achievement of ideal growth conditions. It is not clear what the effects of step bunching would be, but a height of $3a$ corresponds to the c lattice parameter so the film orientation might be affected.

Twinning, due to strain relaxation in connection with structural phase transitions, is also common in perovskites. In LaGaO_3 , for example, twinning leads to surface corrugation and reduced critical current density (Miyazawa 1989). Applying uniaxial pressure and passing through the phase transition at $150 \pm 1^\circ\text{C}$ produced single domain substrates 1 cm_2 in size. An alternative approach to circumvent twinning is the development of non-perovskite substrates, such as the K_2NiF_4 structure (Scheel et al 1991).

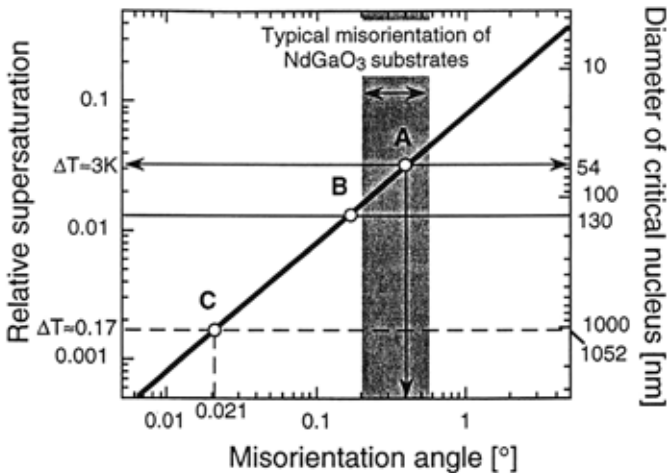


Fig. 11.16. Diameter of critical nucleus with corresponding supersaturation for YBCO on NdGaO_3 , as a function of substrate misorientation angle. *A* represents experimental results, *B* the estimated limit for thin c -oriented films, and *C* the requirement for tunnel devices (Klemenz et al 1999).

There is hope that the development of an optimized substrate, combined with optimized growth and oxidation procedures, will allow single-domain, crack-free HTSC layers with atomically flat surfaces, but this requires intensive efforts to

solve the challenging materials engineering problems. In comparison, the measurement of superconducting properties such as critical temperature and critical current, with its field and temperature dependence, has become routine. It is promising that, in addition to the first groups in Lausanne, Switzerland and Jena, Germany, more groups have begun work in LPE of HTSC, notably in Japan and Cambridge, England.

11.7 Effects of Growth Conditions on Growth Modes

In epitaxy three classical growth modes have been defined by Bauer (1958) from the surface and interfacial free energies: the Stranski-Krastanov (SK) and Volmer-Weber (VW) surface nucleation and growth modes and the Frank-van der Merwe (FVM) layer-by-layer growth. In addition to these classical growth modes, it is necessary to consider additional distinct epitaxial growth modes which can occur under certain conditions (Scheel and Klemens 1996; Scheel 1997). In physical vapor deposition (PVD) and chemical vapor deposition (CVD) of HTSC films, the spiral-island (SI) and screw-island growth mode is observed (Hawley et al 1991, Gerber et al 1991, Lang et al 1992, Nishinaga & Scheel 1996). This mode of growth occurs during the agglomeration phase of the film following initial VW or possibly SK growth. During coalescence, dislocations can be easily generated by accommodation of small translational and rotational displacements between agglomerating islands.

When continuous layer growth occurs in vapor phase epitaxy, after initial growth in the SK, VW or SI mode, a so-called columnar structure may develop. This growth mode is typical for HTSC layers grown from the vapor phase unless a substrate with a large misorientation angle is used. If the angle and direction of misorientation are precisely adjusted, the misorientation steps allow the suppression of two-dimensional nucleation and so of the VW, SK and SI modes. As a result, the columnar growth mode can be suppressed or reduced. The resulting step-flow mode, which is distinct from the FVM mode, allows the attainment of relatively flat surfaces, but at the cost of high step density. The actual step density is similar to that in the VW, SK or SI modes, depending on the supersaturation.

In LPE of YBCO, it is possible to achieve the FVM growth mode, with layer-by-layer growth over macroscopic distances. The distinct feature of this mode is that a new layer is an extremely flat surface, if the substrate and growth parameters are within specified limits. Step bunching may occur at higher supersaturation. The ability to obtain very flat surfaces is the most important distinguishing characteristic of LPE versus vapor growth. A more detailed discussion of epitaxy is given in Appendix B.

An additional growth mode is the leading edge growth mechanism (Scheel & Niedermann 1989) which can occur when leading edges and secondary edges co-exist on narrow side faces and act similarly to elongated dendrite tips. Such leading edge sources can result in fast growth, for example of thin, plate-like crystals, in the same way as the twin-plane re-entrant edge mechanism. This growth mode was identified by a combination of SEM and STM as the mechanism of formation of some plate-like YBCO crystals. The leading edge mechanism is expected to occur at high supersaturation, and therefore not under the conditions necessary for the growth of smooth LPE layers. However in layers grown at intermediate supersaturations there may be competition between layers originating from screw dislocations on the surface and those spreading from the edges.

11.8 Surface Characterization of LPE-grown HTSC layers

The complexity of the cuprate superconductors, including multiple oxygen sites and antisite defects of various kinds, makes the reproducible growth of crystals and layers a serious challenge. Ten or more growth parameters influence the properties of the crystalline product, and the majority of these cannot be controlled adequately. Since the exact replication of material properties cannot be guaranteed, it is important to perform sufficient characterization (in contrast to no or complete characterization- see Scheel et al 1991) as a check on each batch of material. Sufficient characterization is defined as analysis of those chemical and structural aspects that may have an impact on the specific measurement or application. Such characterization may require extensive effort and collaboration, but is necessary both for the interpretation of physical measurements and for the development of HTSC technology, for achieving reproducibility.

For surface characterization of LPE layers, the most important measurement techniques are optical interference microscopy, scanning tunnel microscopy (STM) and atomic force microscopy (AFM). Differential interference optical microscopy (DIM), especially using the Nomarski technique, has become the normal tool for routine characterization of the surface of LPE-grown HTSC layers with large interstep distances. The technique is described in Chapter 8 together with some examples of its application to the surface of bulk crystals.

Fig. 11.17 shows the detection limits of the most important microscopy techniques together with observed step heights and interstep spacings for PVD-, CVD- and LPE-grown layers. Also shown are the inherent limits of PVD processes and the practical limits of LPE interstep distances.

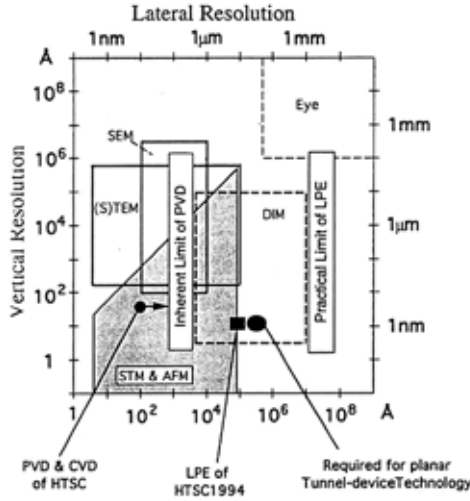


Fig. 11.17. Vertical and lateral resolution of scanning tunnel microscopy (STM) and differential interference contrast microscopy (DIM), with inherent limit of vapor deposition and practical limit of LPE, also step distances required for HTSC tunnel device technology (Scheel 1994).

In Fig. 11.18 an AFM image is shown of a macrospiral formed during LPE growth of a c-axis YBCO film on (110) NdGaO₃ (Klemenz 1998). The lattice mismatch in this case is less than 0.2% at the growth temperature, and the supersaturation about 3%. This layer contains numerous growth spirals, and has been partly oxidized. Some dislocations with non-elementary step heights were also observed. Fig.11.18a shows a single-core spiral with steps that are composed of seven bunched steps. In Fig.11.18b the height scan across these steps is shown. The interstep distance is about 2.9 μm.

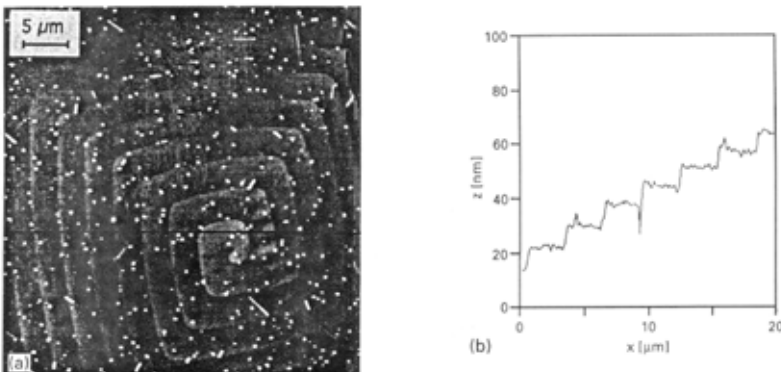


Fig. 11.18. (a) AFM image of a macrospiral grown on a c-axis oriented YBCO layer. Interstep distance is about 2.9 μm. (b) Height scan along the steps shows a step height of 7 YBCO cells of 1.2nm.

Fig. 11.19 shows data from AFM measurements of a number of spirals to determine the relationship between interstep distance and step height. For the solid line, the interstep distance increases as the total height increases. Extrapolation to a single step gives the interstep distance for a single spiral as 0.435 nm, corresponding to a critical nucleus of 0.023 nm. For groups of S dislocations, the interstep distance decreases with S as expected from the BCF theory. The two spirals labelled A and B in the Figure have $m=2$, $S=6$ and $m=4$, $S=3$ respectively (with m the multiplicity), each having a hollow core of about 1 μm diameter.

For the spirals for which measurements were possible, the interstep distance is given by

$$\gamma_0 = 19 \gamma_m a m / \epsilon k T \sigma. \quad (11.2a)$$

with the factor ϵ given by

$$2\pi r^* S / L < \epsilon < S/2 \quad (11.2b)$$

For the investigated surface, the interstep distance increases as the total height of bunched steps increases. The measured step density is about 22,500 per cm. The approximate constancy of the step density over the surface, in spite of variation in interstep distance, is evidence for diffusion-limited growth.

Hollow cores of various size and shape have been observed in HTSC LPE layers and on layers grown by vapor deposition. The perimeter of cores in LPE appears never to exceed 2 μm .

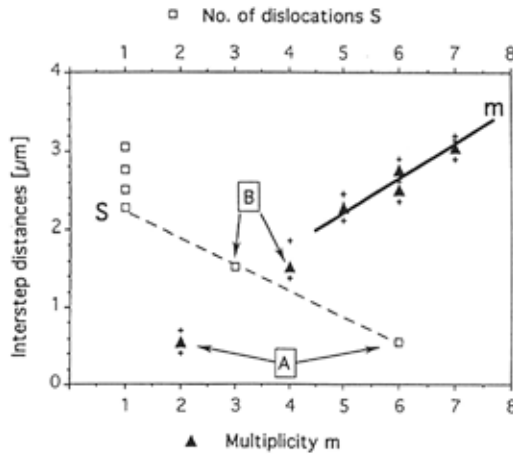


Fig. 11.19. Measured macrostep distances of macrospirals as a function of multiplicity m and number of turns S originating from the core. For single dislocations, interstep distance increases with m , but for complex sources it decreases by a factor ϵ (A and B) (Klemenz 1998).

11.9. Summary

The discovery of high- T_c superconductivity in 1987 raised the hope for a new era in technology.

Breakthroughs were envisaged in the fields of energy, in the form of electric current transport and storage, current limiters and fusion, transport (trains and ships), detectors for medicine and biology, and in fast electronic switching. However, over a decade after the discovery, the extremely complex materials engineering problems have been relatively neglected. Despite the initially enormous efforts and support from industry and governments, HTSC has found only minor niche applications so far. Instead of a new era and revolution based on HTSC, this phenomenon remains largely a physical curiosity. In this chapter an attempt has been made to review some of the major difficulties of crystal growth and epitaxy of HTSC compounds. Their thermodynamic stability limits narrow the experimental parameter ranges available to the crystal grower to such an extent that preparation of high-quality crystals and layers still is not impossible, but requires detailed knowledge and skill in crystal growth and epitaxy technology. Also it is clear that sufficient control of the growth process is possible only in crystal growth from high-temperature solutions and in liquid phase epitaxy: only very near to thermodynamic equilibrium can compact epitaxial layers with the required flat surfaces be expected, with minimum bulk defects for maximum percolation of superconducting current. In contrast, large numbers of localized defects are required as pinning centers for the superconducting vortices in order to achieve higher current densities, much higher than those achieved to date, which correspond to about 1% of the theoretical value. The achievement of such local defects is a challenging topic which could not be discussed here.

The fabrication of HTSC crystals and epitaxial layers involves numerous growth parameters, a few of which have been discussed in this chapter and throughout the book. Several of these parameters cannot be controlled with sufficient precision at this time so that the growth processes are not reproducible. Therefore, each crystal, each layer, even from the same laboratory, is different: *no two crystals are alike*. From this it is clear that physical measurements on crystals and layers characterized only by their origin (laboratory or crystal grower, Stupp and Ginsberg 1992) are of marginal value.

The narrow thermodynamic stability limits of the HTSC compounds, the different chemical bonds within the sensitive structures, and the complex composition on the one hand, and the difficulty of appropriate control of the growth parameters on the other hand, lead to a high probability of growth defects. Besides the *chemical polytypism* mentioned above, there are frequently inclusions of other phases like non-dissolved constituent oxides, reaction products from crucible corrosion, neighbour phases from the phase diagram, or solidified sol-

vent due to growth instability. Furthermore, stacking faults, grain boundaries, antiphase boundaries, and twins are often observed as are edge and screw dislocations. Other differences of HTSC crystals and layers may be due to different site occupancies (e.g. NdBa replacement), due to the oxygen content and distribution or oxygen ordering effects, and due to all kinds of point defects including impurities substituting for the constituent HTSC cations. This large variety of defects will not be observed in all crystals and layers as one would expect systematic relationships of defect formation with the growth method and with the growth conditions which, however, have not been investigated so far.

Many of the listed defects will have an impact on the superconducting properties. Therefore, for serious physical measurements the characterization of all those chemical and structural defects is required which have or may have an influence on the specific physical measurement or application. This minimum requirement is defined as "*sufficient characterization*" (Scheel et al. 1991), in contrast to complete characterization describing all deviations from the ideal crystal. For real progress in understanding the phenomenon of high-temperature superconductivity it is necessary that solid-state chemists, crystallographers and physicists together analyze and predict the role of individual defects so that rules of sufficient characterization for specific physical HTSC measurements can be established. This will also help to develop and optimize growth processes for crystals and layers which are suitable for physical investigations and for applications of HTSC.

It is hoped that after the initial hectic decade plus in studying the physics of HTSC, there will be a serious focus on progress in understanding the materials problems of these interesting materials, as an essential for realizing their great potential for important applications.

References

- Abrikosov A. A. (1988), Summer School on High- T_c Superconductivity, El Escorial, Spain, July 1988, private communication.
- Adachi, S., Tokiwa-Yamamoto, A., Itoh, M., Isawa, K. and Yamauchi, H. (1993) *Physica C* **214**, 313.
- Aichele, T., Bornmann, S., Dubs, C. & Gornert, P. (1997) *Cryst. Res. Technol.* **32**, 1145.
- Alexander, K. B., Goyal, A., Kroeger, D. M., Selvamanickam, V. and Salama, K. (1992) *Phys. Rev. Lett.* **45**, 2331.
- Antipov, E. V., Loureiro, S. M., Chaillout, C., Capponi, J. J., Bordet, P., Tholence, J. L., Putilin, S. N. and Marezio, M. (1993) *Physica C* **215**, 1 (see also *Physica C* **235-240**, 1994, 21).
- Assmus, W. and Schmidbauer, W. (1993) *Supercond. Sci. Technol.* **6**, 655.
- Bardeen, J., Cooper, L. N. and Schrieffer, J. R. (1957) *Phys. Rev.* **108**, 162, 1175.
- Bednorz, J. G. and Mueller, K. A. (1986) *Z. Phys.* **B64**, 189.
- Berkowski, M., Bowen, P., Liechti, T. and Scheel, H. J. (1992) *J. Amer. Ceram. Soc.* **75**, 1005.
- Bormann, R. and Nolting, J. (1989) *Appl. Phys. Lett.* **54**, 2148.
- Boutellier, R., Sun, B. N., Scheel, H. J. and Schmid, H. (1989) *J. Crystal Growth* **96**, 465.
- Calestani, G., Rizzoli, C. and Andretti, G.D. (1987) *Solid State Comm.* **66**, 223.
- Cava, R. J. (1990) *Science* **247**, 656.
- Chu, S. and Mc Henry, M. E. (1997)
- Chu, S., Wang, X., Cheng, X., Wang, J. and Chu, S. (1992) *Eng. Chem. & Met.* **13**, 211.
- Ciszek, T. F., Goral, J. P., Evans, C. D. and Katayama - Yoshida, H. (1988) *J. Crystal Growth* **91**, 312.
- Colson, D., Bertinotti, A., Hammann, J., Marucco, J. F. and Pinatel, A. (1994) *Physica C* **233**, 231.
- Duan, H. M., Kaplan, T. S., Dlugosch, B., Herman, A. M., Swope, J., Drexler, J., Boni, P. and Smyth, J. (1992) *Physica C* **203**, 257.
- Erb, A., Walker, E. and Fluekiger, R. (1996) *Physica C* **258**, 9.
- Dubs, C., Schuler, T., Bruchlos, G., Zeisberger, M. & Gornert, P. (1995) *J. Crystal Growth* **156**, 216.
- Feigelson, R. S., Gazit, D., Fork, D. K. and Geballe, T. H. (1988) *Science* **240**, 1642 and title page of June 1988 issue of Science.
- Finger, L. W., Hazen, R. M., Downs, R. T., Meng, R. L. and Chu, C. W. (1994) *Physica C* **226**, 216.
- Francois, M. and Scheel, H. J. (1989) *J. Less Common Metals* **150**, 211.
- Gai, P.L. and Thomas, J. M. (1992) *Superconductivity Review* **1**, 1.
- Gazit, D. and Feigelson, R. S. (1988) *J. Crystal Growth* **91**, 318.
- Gerber, C., Anselmetti, D., Bednorz, J. G., Mannhart, J. & Schlom, D. G., (1991) *Nature* **350**, 279.
- Ginley, D. S., Morosin, B., Baughman, R. J., Venturini, E. L., Schirber, J. E. and Kwak, J. F. (1988) *J. Crystal Growth* **91**, 456.
- Givargizov, E. I., Sheftal, N. N. and Klykov, V. I. (1982) *Current Topics in Materials Science* (North Holland, Amsterdam) **10**, 1.
- Grabow, M.H. & Gilmer, G. H., (1988) *Surface Sci.* **194**, 333.
- Goodenough, J. B. (1990) *Supercond. Sci. Technol.* **3**, 26.
- Hallstedt, B., Risold, D. and Gauckler, L. J. (1996) in Proc. *Workstoffwoche* 96, (May 28-31, 1996), DGM, Oberursel, Germany, preprint 7.11.1996.
- Hashimoto T., Koinuma H. and Kishio K. (1991) *Japan. J. Appl. Phys.* **30**, 1685.
- Hawley, M., Raistrick, I. D., Beery, J. G. & Houlton, R. J., (1991) *Science* **251**, 1587.
- Hidaka, Y., Oda, M., Suzuki, M., Maeda, Y., Enomoto, Y. and Murakami, T. (1988) *Japan. J. Appl. Phys.* **27**, L538.
- Hikita, M., Iwata, T., Tajima, Y. and Katsui, A. (1988) *J. Crystal Growth* **91**, 282.
- Hinks, D. G., Soderholm, L., Capone II, D. W., Jorgensen, J. D., Schuller, I. K., Segre, C. U., Zhang, K. and Grace, J. D. (1987) *Appl. Phys. Lett.* **50**, 1688.
- Holba P. (1992) *Czech. J. Phys.* **42**, 549.
- Holba, P. and Scheel, H. J., submitted.
- Huang, Y., Huang, M.-H., Yeh, K.-W. and Hong, M.-Y. (1995) *Mater. Chem. Phys.* **41**, 290.

- Jin, S., Tiefel, T. H. and Sherwood, R. C. (1988) *Appl. Phys. Lett.* **54**, 6.
- Jorgensen, J. D. (1987) *Japan. J. Appl. Phys.* **26** Suppl., 2017.
- Kaiser, D. L., Holtzberg, F., Scott, B. A. and McGuire, T. R. (1987) *Appl. Phys. Lett.* **51**, 1040.
- Kaiser, D. L., Holtzberg, F., Chisholm, M. F. and Worthington, T. K. (1987) *J. Crystal Growth* **85**, 593.
- Katsui, A. and Ohtsuka, H. (1988) *J. Crystal Growth* **91**, 261.
- Klemenz, C. (1998) *J. Crystal Growth* **187**, 221.
- Klemenz, C. and Scheel, H. J. (1993), *J. Crystal Growth* **129**, 421.
- Klemenz, C. and Scheel, H. J. (1996), *Physica C* **265**, 126.
- Klemenz C. & Scheel, H.J. (1999) *J. Crystal Growth* **200**, 435 and 203, 534.
- Klemenz, C., Utke, I. & Scheel, H.J., (1999) *J. Crystal Growth* **204**, 62.
- Komatsu, H., Kato, Y., Miyashita, S. and Inoue, T. (1992) Extended Abstracts of the International Workshop on Superconductivity, Honolulu / Hawaii June 23 - 26, 1992, p. 93.
- Kotani, T., Kaneko, T., Takei, H. and Tada, K. (1989) *Japan. J. Appl. Phys.* **28**, L1378.
- Kuroda, K., Choi, I., Unoki, H. and Koshizuka, N. (1997) *J. Crystal Growth*,
- Laligant, Y., Ferey, G., Hervieu, M. and Raveau, B. (1987) *Europhys. Lett.* **4**, 1023.
- Lang, H.P., Haefke, H., Leemann, G. & Guntherodt, H. J. (1992) *Physica C* **194**, 81.
- Laudise, R. A., Schneemeyer, L. F. and Barns, R. L. (1987) *J. Crystal Growth* **85**, 569.
- Licci, F., Besagni, T., Frigeri, C., Paris, C., Aquilano, F. and Scheel, H. J. (1991a) *Proc. 3rd Europ. Conf. Crystal Growth*, Budapest May 5-11, 1991.
- Licci, F., Frigeri, C. and Scheel, H. J. (1991b) *J. Crystal Growth* **112**, 606.
- Licci, F., Scheel, H. J. and Tissot, P. (1991c) *J. Crystal Growth* **112**, 600.
- Lindemer, T. B., Washburn, F. A., Mac Dougall, C. S., Feenstra, R. and Cavin, O. B. (1991) *Physica C* **178**, 93.
- Liu, J. Z., Crabtree, G. W., Rehn, L. E., Geiser, U., Young, D. A., Kwok, W. K., Baldo, P. M., Williams, J. M. and Lam, D. J. (1988) *Physics Lett. A* **127**, 444.
- Liu, R. S., Zhou, W., Cooper, J. R., Bennett, M. J., Janes, R., Zheng, D. N. and Edwards, P. P. (1990) *Supercond. Sci. Technol.* **3**, 568.
- Luo L., Hawley, M. E., Maggiore, C. E., Dye, R. C., Muenchausen, R. E., Chen, L., Schmidt, B. & Kaloyeros, A.E. (1993) *Appl. Phys. Lett.* **62**, 485.
- Matsubara, I., Kageyama, H., Tanigawa, H., Ogura, T., Yamashita, H. and Kawai, T. (1989) *Japan. J. Appl. Phys.* **28**, L 1121.
- Miyazawa, S. (1989) *Appl. Phys. Lett.* **55**, 2230.
- Miyazawa, S. & Mukaida, M. (1994) *Appl. Phys. Lett.* **64**, 2160.
- Moiseev, G. K., Vatolin, N. A., Zaizeva, S. I., Ilynych, N. I., Tsagerishvili, D. S., Gvelesiani, G. G., Baratashvili, I. B. and Sestak, J. (1992) *Thermochim. Acta* **198**, 267.
- Morosin, B., Ginley, D.S., Venturini, E.L., Hlava, P.F., Baughman, R.J., Kwak, J. F. & Schirber, J.E. (1988) *Physica C* **152**, 223.
- Murakami, M. (1992) *Supercond. Sci. Technol.* **5**, 185.
- Nishinaga, T. & Scheel, H. J., (1996) in *Advances in Superconductivity VIII* (Ed. H. Hayakawa & Y. Enomoto), Springer, Tokyo, p. 33.
- Nomura, S., Yamashita, T., Yoshino, H. and Ando, K. (1988) *Japan. J. Appl. Phys.* **27**, L 1251.
- Oka, K. and Unoki, H. (1987) *Japan. J. Appl. Phys.* **26**, L1590 ; see also *J. Crystal Growth* **99**, 922 (1990).
- Paranthaman, M., Duan, H. M. and Herman, A. M. (1992) in *Thallium - based high - temperature superconductors*, editors A. M. Herman and J. V. Yakhmi, Dekker, New York.
- Putilin, S. N., Bryntse, I. and Antipov, E.V. (1991) *Mater. Res. Bull.* **26**, 1299.
- Putilin, S. N., Antipov, E. V., Chmaissem, O. and Marezio, M. (1993a) *Nature* **362**, 226.
- Putilin, S. N., Antipov, E. V. and Marezio, M. (1993b) *Physica C* **212**, 266.
- Rao, C. N. R. (1988) *Mod. Phys. Lett.* **2**, 1217.
- Raveau, B., Michel, C. and Hervieu, M. (1990) *J. Solid State Chem.* **88**, 140.
- Ren, Z., Yan, X., Jiang, Y. and Guan, W. (1988) *J. Crystal Growth* **92**, 677.

- Revcolevschi, A. and Jegoudez, J. (1996) in "Coherence in High Temperature Superconductors", editors G. Deutscher and A. Revcolevschi, World Scientific, Singapore 1996, 19-41.
- Roth, R. S., Davis, K. L. and Dennis, J. R. (1987) *Adv. Ceram. Mater.* **2**, 303.
- Rothman, S.J., Routbort, J. L., Welp, U. & Baker, J. E. (1991) *Phys. Rev. B.* **44**, 2326.
- Rytz, D. and Scheel, H. J. (1982) *J. Crystal Growth* **59**, 468.
- Sadowski, W. and Scheel, H. J. (1989) *J. Less-Common Metals* **150**, 211.
- Sandiumenge, F., Dubs, C., Gornert, P. & Gali, S. (1994) *J. Appl. Phys.* **75**, 5243.
- Scheel, H. J. (1988) *Physica C* **153-155**, 44.
- Scheel, H. J. (1994) *MRS Bulletin* **19** No 9,26.
- Scheel, H.J., 1997, Proc. Intl. Symp. Laser & Non-linear Optical Materials, IS-LNOM '97, Singapore, Nov. 3-5, 1997, Ed. T. Sasaki, Data Storage Inst., Singapore.
- Scheel, H. J. & Klemenz, C. (1996) *Electrochem. Soc. Proc.* **11**, 20.
- Scheel, H. J. and Licci, F. (1987) *J. Crystal Growth* **85**, 607.
- Scheel, H. J. and Licci, F. (1988) in MRS Proc. 99, editors M. B. Brodsky, R. C. Dynes, K. Kitazawa and H. L. Tuller (MRS 1987 Fall Meetg. Boston Nov. 30-Dec. 5, 1987), 595.
- Scheel, H. J. and Licci, F. (1991), *Thermochim. Acta* **174**, 115.
- Scheel, H. J. and Niedermann, Ph. (1989) *J. Crystal Growth* **94**, 281.
- Scheel, H. J., Binnig, G. & Rohrer, H. (1982) *J. Cryst. Growth* **60**, 199.
- Scheel, H. J., Sadowski, W. and Schellenberg, L. (1989) *Supercond. Sci. Technol.* **2**, 17.
- Scheel, H. J. Berkowski, M. and Chabot, B. (1991) *J. Crystal Growth* **115**, 19.
- Scheel, H.J., Klemenz, C., Reinhart, F-K., Lang, H. P. & Guntherodt, H-J. (1994) *Appl. Phys. Lett.* **65**, 901.
- Schilling, A., Cantoni, M., Guo, J. D. and Ott, H. R. (1993) *Nature* **353**, 56.
- Schmid, H. (1988) private communication.
- Schneemeyer, L. F., Waszczak, J. V., Siegrist, T., van Dover, R. B., Rupp, L. W., Batlogg, B., Cava, R. J. and Murphy, D. W. (1987) *Nature* **328**, 601.
- Schneemeyer, L. F., Van Dover, R. B., Glarum, S. H., Sunshine, S. A., Fleming, R. M., Batlogg, B., Siegrist, T., Marshall, J. H., Waszczak, J. V. and Rupp, L. W. (1988) *Nature* **332**, 422.
- Schwer, H., Karpinski, J., Conder, K., Lesne, L., Rossel, C., Morawski, A., Lada, T. and Paszewin, A. (1995) *Physica C* **243**, 10.
- Siegrist, T., Schneemeyer, L. F., Waszczak, J. V., Singh, N. P., Opila, R. L., Batlogg, B., Rupp, L. W. and Murphy, D. W. (1987) *Phys. Rev. B* **36**, 8365.
- Siegrist, T. et al. (1992) *Appl. Phys. Lett.* **60**, 2488.
- Sleight, A. W. (1988) *Science* **242**, 1519.
- Stacy, A. (1989), private communication.
- Stowell, M. J. (1975) in Epitaxial Growth, Part B (Ed. J. W. Matthews), Academic Press, Ch. 5.
- Takekawa, S., Nozaki, H., Umezono, A., Kosuda, K. and Kobayashi, M. (1988) *J. Crystal Growth* **92**, 687.
- Thomson, C., Cardona, M., Gegenheimer, B., Liu, R. and Simon, A. (1988) *Phys. Rev. B* **37**, 9860.
- Tsagareishvili, D. S., Gvelesiani, G. G., Baratashvili, I. B., Moiseev, G. K. and Vatin, N. A. (1990) *Russ. J. Phys. Chem.* **64**, 1404.
- Venturini, E. L., Tigges, C. P., Baugham, R. J., Morosin, B., Barbour, J. D., Mitchell, M. A. and Ginley, D. S. (1991) *J. Crystal Growth* **109**, 441.
- Voronin, G. F. and Degterov, S. A. (1991) *Physica C* **176**, 387.
- Wang, J., Monot, I. and Desgardin, G. (1996) *J. Mater. Res.* **11**, 2703.
- Wu, M. K., Ashburn, J. R., Torng, C. J., Hor, P. H., Meng, R. L., Huang, C. J., Wang, Y. Q. and Chu, C. W. (1987) *Phys. Rev. Lett.* **58**, 908.
- Yamada, Y. and Shiohara, Y. (1993) *Physica C* **217**, 182.
- Zhokhov, A. A. and Emelchenko, G. A. (1993) *J. Crystal Growth* **129**, 786.